nzsee
NEW ZEALAND SOCIETY FOR EARTHQUAKE ENGINEERING

Evaluation of assessment approaches for soil-foundation-structure interaction of frame buildings

M.D.L. Millen & M. Cubrinovski
Department of Civil and Natural Resources Engineering, University of Canterbury, Christchurch.

ABSTRACT

The consideration of soil and foundation deformations within the seismic assessment of buildings can be critical for evaluating the likely load paths and consequent deformations. Frame buildings provide numerous complexities for estimating the soil-foundation load-deformation behaviour, due to the redistribution of vertical load that occurs between footings during seismic excitation. Our research study examines various approaches for soil-foundation-structure interaction (SFSI) analysis with specific reference to their applicability to practice. This paper provides guidance on the development, validation and implementation of beam on nonlinear Winkler foundation (BNWF) models for modelling the soil-foundation interface in the seismic assessment of frame buildings.

This paper uses a series of numerical studies to evaluate the expected load paths on soil-foundation interfaces, to optimise the modelling of the initial rotational and vertical stiffness, and to validate the modelling of the moment-rotation behaviour, moment capacity and vertical load versus settlement. A four storey building is simulated under a push-pull analysis under fixed base conditions, and compared to corresponding simulations that account for the soil-foundation deformations. The role of SFSI in the push-pull seismic assessment is apparent, with the global foundation rotation and deformations resulting in a clear change in the overall development of base shear. The local footing deformations also changed the moment demands that developed within the top of the ground floor columns, increasing the potential for a soft storey mechanism.

1 INTRODUCTION

New Zealand's building stock is largely located on soil deposits where soil and foundation deformations can significantly modify the building response compared to fixed base conditions. Conventional linear analysis of simple soil-structure systems shows that soil flexibility leads to an elongation in vibration period and generally reduces distortion of the superstructure. However, for more complex systems that have appreciable inelastic deformation in the soil, superstructure and/or soil-foundation interface, soil-foundation-structure interaction

(SFSI) can produce detrimental changes to the system response. The 2010-2011 Canterbury earthquake sequence provided numerous examples of significant soil and foundation deformation that led to buildings being deemed economically irreparable (Cubrinovski et al., 2011).

The NZSEE seismic guidelines (MBIE et al., 2017), recommend evaluating SFSI through simple hand-calculations checks (e.g. Millen et al., 2016 [updated in Millen et al. (2020)]) and/or simulating the building using numerical analysis and modelling the soil-foundation interface with a beam on nonlinear Winkler foundation (BNWF) model, and in extreme cases modelling the soil using nonlinear finite element analysis.

The goal of this paper is to first provide guidance on simulating soil-foundation interfaces for frame buildings using a BNWF model, and second, to better understand the effects of SFSI on frame buildings. In this paper the authors first present an investigation of the expected load paths for a soil-foundation interface, then several validation studies are performed to understand the limitations of BNWF models, and finally the results of several push-pull analyses of a 4-storey frame building under different conditions are presented.

2 ESTIMATION OF LOAD PATHS

Isolated footings in a frame building undergo complex load paths during seismic loading due to the variations in both axial and moment demands. Figure 1 demonstrates the key mechanisms that control the footing loads. During an earthquake, the axial load in exterior footings cyclically increases and decreases due to frame action, and moment demand cyclically varies. However, if all the beams yield then the change in axial load is limited, and if the column base yields then the increase in moment demand is also capped. The interior columns experiences an increase in moment demand with increased drift until the column base yields. While the load path is reasonably moment-dominant, there can be some redistribution of axial load due to the plastic deformation in the beam hinges. Furthermore, yielding in the soil and uplift of the footing can additionally limit the development of moment demand in the footing, while tie beams act to resist foundation deformation.

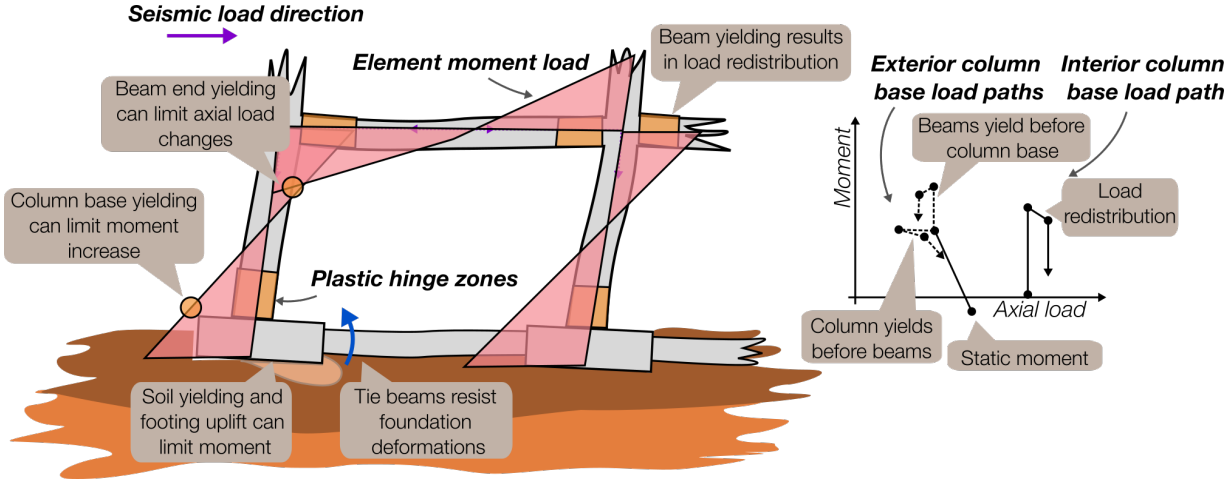

Figure 1: Footing load paths

To evaluate the expected load paths of footings, two reinforced-concrete frame buildings (4 storey and 8 storey) have been designed using the displacement-based design approach assuming fixed base conditions (Sullivan et al., 2012). The buildings have a constant interstorey height of 3.4 m and two 4 m bays. The floor out-of-plane width per frame is 4 m, and in-plane length of 12 m, with an assumed applied floor load of 8 kPa for all loading scenarios. The concrete crushing capacity was assumed to be 30 MPa and reinforcing steel yield strength of 300 MPa. The footings were designed to be all the same size, based on the vertical load from the full tributary area and 8 kPa applied load. The foundation design achieved a factor of safety of three against bearing capacity failure according to the method from Salgado (2008) adopting the depth and shape factors from Brinch Hansen (1970). The concrete unit weight for the footing was assumed to be 23 kN/m^3, and soil

internal frictional angle was 35° and unit weight of 17 kN/m^3. The design drift was 2%, and the design spectrum corner displacement and period were 0.4 m and 4 s respectively. The design moments for the beams at the column faces, and column bases, were determined using the moment redistribution method where the column inflexion point in the ground floor was assumed to be at 0.6 of the height. A summary of the design inputs and outputs are given in Table 1.

Table 1: Summary of the design inputs and outputs for a 4-storey and 8-storey building

Property	**4-storeys**	**8-storeys**
Beam depths [m]	0.43	0.51
Beam widths [m]	0.33	0.275
Column depths/widths [m]	0.43	0.51
Footing length/width [m]	1.25	1.5
Footing depth [m]	1.2	1.6
Column base moments [kNm]	182	184
Beam design moments [bottom to top] [kNm]	231;231;138;138	270; 270; 239; 239; 181; 181; 100; 100

An estimate of the moment demand on each footing at the design drift was achieved by extrapolating the column base moment down to the base of the footing. The vertical load on the footings was estimated by combining the static axial load (including footing mass) with the vertical load from seismic frame action. The symmetric demands at peak drift in both directions have been plotted in Figure 2 in normalised axial load, Q_N, and normalised moment, Q_M, space. Q_N is the vertical load divided by the ultimate bearing capacity and Q_M is moment demand divided by the ultimate bearing capacity and footing in-plane length. The ultimate bounding surfaces from Figini et al. (2012) and Gottardi and Butterfield (1993) are shown, as well as the range of uplift limits depending on soil nonlinearity for a strip footing from Cremer et al. (2001).

Assuming that there are no tie beams to resist the moment and axial loads, the footing demands at the frame design drift would significantly exceed the footing resistance capacity from both Figini et al. (2012) and Gottardi and Butterfield (1993). While this is a simplistic estimation of the load paths, it highlights that footings can experience significant variation in both axial load and moment demand. Therefore, a realistic simulation of footing behaviour needs to capture:

1. The initial vertical and rotational stiffness of the soil-foundation interface
2. The foundation uplift, moment capacity and the nonlinear moment-rotation response of the footing at different levels of axial load
3. The vertical load versus deformation relationship
4. The hysteretic energy dissipation

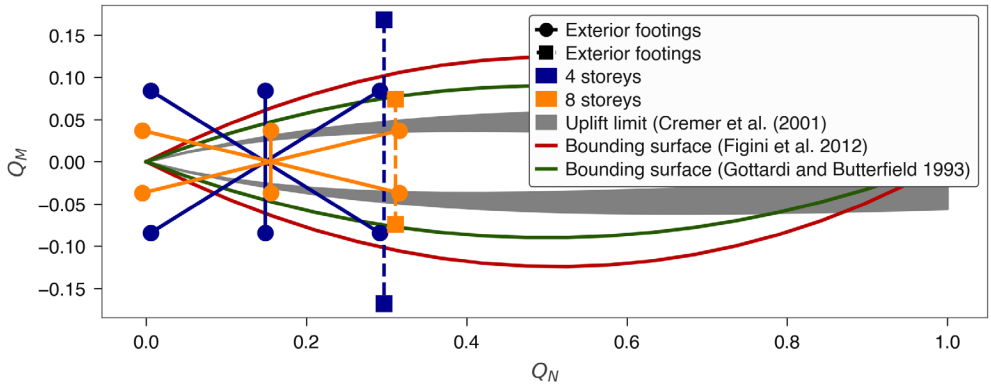

Figure 2: Estimation of footing load paths based on fixed base design assuming no tie beams

3 SOIL-FOUNDATION INTERFACE MODELLING USING BNWF

While there are several options for modelling soil-foundation interfaces (e.g. soil finite element mesh, macro-element models), perhaps the most widely adopted method is the beam on nonlinear Winkler foundation (BNWF). The BNWF consists of a set of independent nonlinear vertical springs distributed along the base of a foundation element (Figure 3 illustrates some of the key features).

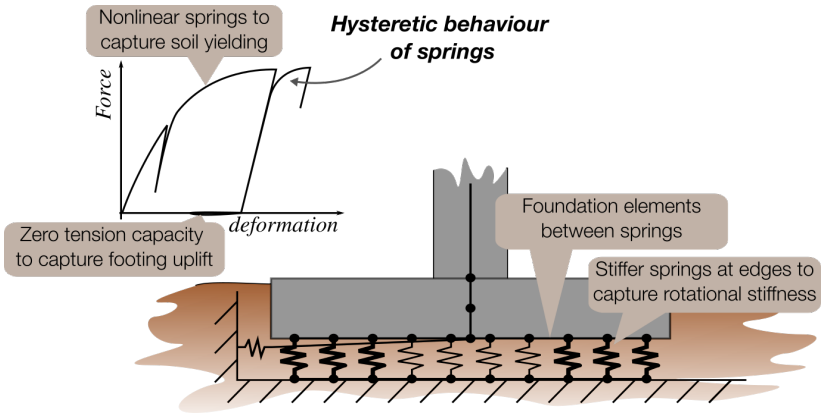

Figure 3: Key aspects of the BNWF model

The BNWF is computationally faster than the finite-element modelling approach, and can be implemented using uniaxial spring elements that are typically available in structural analysis software. Whereas macro-element models require moment-axial-shear dependent spring elements and appropriate constitutive relationships between the modes of deformation. While the BNWF model can sufficiently capture the response for load paths that remain in the linear range and are either moment or vertical load dominated, there can be significant deficiencies when considering load paths in the nonlinear range that must simultaneously deal with variations in vertical and moment load. To allow this modelling approach to be applied within a numerical pushover analysis of a frame building for seismic assessment, the simulation criteria outlined in the previous section need to be met. To scrutinise these criteria, a set of small studies were performed to develop a BNWF model using widely available nonlinear springs and compared it to the performance of existing BNWF models. Note that the hysteretic energy dissipation and estimation of residual deformation have not been investigated here, however, they are part of a wider study currently being performed by the authors. Furthermore, shear deformation at the soil-foundation interface has not been addressed and is assumed to be zero in all of the models presented in this paper.

3.1 Calibration of the initial vertical and rotational stiffness

One of the fundamental aspects of the foundation response is the modelling on the initial vertical and rotational stiffness, which control the amount of global foundation rocking and local footing rotation under low levels of loading. Unfortunately the use of only vertical springs distributed across the foundation area cannot capture the full range of theoretical rotational and vertical stiffnesses from Gazetas (1991). The vertical stiffness, K_N, and rotational stiffness about the length ($K_{M,length}$) and width $K_{M,width}$) axes, for rectangular footings with no embedment from Gazetas (1991) are given in Eq 1, 2 and 3 respectively. G is the soil shear modulus, v is the Poisson's ratio, b and l are equal to half the foundation length and width respectively, I_{bx} and I_{by} are the area moment of inertia around the length and width axes, and k_n and k_m are frequency dependent factors.

$$K_N = \frac{2Gl}{(1-v)}\left[0.73 + 1.54\left(\frac{b}{l}\right)^{0.75}\right]k_n \quad (1)$$

$$K_{M,length} = \frac{G}{(1-v)} I_{bx}^{0.75}\left(\frac{l}{b}\right)^{0.25}\left[2.4 + 0.5\frac{b}{l}\right]k_m \quad (2)$$

$$K_{M,width} = \frac{G}{(1-v)} I_{by}^{0.75}\left[3\left(\frac{l}{b}\right)^{0.15}\right]k_m \quad (3)$$

Assuming a stiffness intensity (k_s, spring stiffness per unit area, also known as the subgrade reaction coefficient), then for an infinite number of springs the vertical stiffness and rotational stiffness around the out-of-plane length, L_{oop}, for a BNWF can be defined from Eq 4 and Eq 5, where L_{ip} is the in-plane length and x and dx are the distance from the foundation centre, and an increment along the in-plane axis respectively.

$$K_{N,BNWF} = \int_{-\frac{L_{ip}}{2}}^{\frac{L_{ip}}{2}} k_s\, dx \cdot L_{oop} \quad (4)$$

$$K_{M,BNWF} = \int_{-\frac{L_{ip}}{2}}^{\frac{L_{ip}}{2}} k_s \cdot x^2\, dx \cdot L_{oop} \quad (5)$$

Assuming the stiffness intensity is parabolic (Eq 6), then the spring distribution coefficients a and c can be computed using Equations 7 and 8 respectively, based only on the dimensionless property $\mathbb{k}$ (Eq 9). However, c represents the stiffness intensity at the centre of the footing, and if $\mathbb{k}$ exceeds 0.15, then c provides a negative stiffness! Therefore for foundations that have $\mathbb{k}$ greater than 0.15, a compromise must be made for a parabolic spring distribution. Note that the most extreme spring distribution of allocating all the stiffness intensity to the very edges of the footing (i.e. a two spring model), increases the $\mathbb{k}$ limit to 1/4, however, this distribution cannot accurately reproduce other aspects of the response (e.g. footing uplift). Other options include using an additional rotational spring (e.g. Wotherspoon, 2009), or out-riggers where the springs extend beyond the foundation width, however, both these options limit the ability of the BNWF to capture the foundation moment capacity. Partially due to the inconsistency of the distribution of stiffness, it should be recognised that the demands that develop within the foundation elements of the BNWF do not represent the actual demands that would develop within the foundation, and should not be used for designing the foundation reinforcement.

$$\frac{k_s}{K_N/(L_{ip}\cdot L_{oop})} = a\left(\frac{x}{L_{ip}}\right)^2 + c \quad (6)$$

$$a = 180\,\mathbb{k} - 15 \quad (7)$$

$$c = \frac{9}{4} - 15\,\mathbb{k} \quad (8)$$

$$\mathbb{k} = \frac{K_M}{K_N \cdot L_{ip}^2} \quad (9)$$

To provide reasonable behaviour for a wide range of situations, Eq 6 should be used up until $\mathbb{k}$ = 0.143 (c = 0.1). At higher $\mathbb{k}$, keep c = 0.1, and adjust a to match either the rotational stiffness using Eq 10, or set a equal to 10.8 to match the vertical stiffness, or interpolate between the two values depending on the expected load path.

$$a = 80\,\mathbb{k} - 2/3 \quad \textit{[Match rotational stiffness]} \qquad (10)$$

Figure 4a and b shows the ratio of the BNWF versus theoretical stiffness values for the different presented options, as well as the ratios when applying the ATC-40 (2008) BNWF model. While all options provide reasonable estimates of both the vertical and rotational stiffness when $\mathbb{k}$ is less than 0.2, the ATC-40 and the 'Match KN' option result in a significant deviation of rotational stiffness at high values of $\mathbb{k}$, while matching the rotational stiffness results in an overestimation of vertical stiffness. Figure 4c shows the change in $\mathbb{k}$ as the ratio L_{oop}/L_{ip} increases, (which tends to a theoretical value of 0.54 for a strip footing) using impedance equations from Gazetas (1991) (Eq 1, 2 and 3). The parabolic and two spring limits are also shown on Figure 4c, highlighting that even for square footings the parabolic model does not adequately match the stiffness in both modes of deformation.

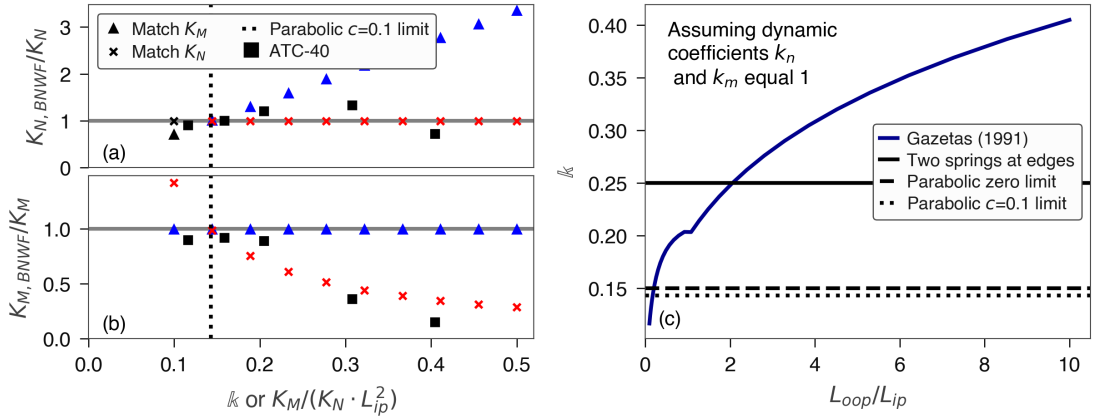

Figure 4: BNWF stiffnesses versus theoretical values a) vertical stiffness comparison, b) rotational stiffness comparison c) variation of $\mathbb{k}$ with geometry

3.2 Capture foundation uplift, moment capacity and the nonlinear moment-rotation response of the footing at different levels of axial load

To evaluate the moment-rotation performance of BNWF models, a series of simple push-pull analyses were performed in OpenSees (McKenna et al., 2010) and O3seespy and extension library of OpenSeesPy (Zhu et al., 2018). A BNWF foundation with 20 springs was attached to a 5 m vertical element, where a horizontal load was applied. The foundation was 1 m by 1 m and had a depth of 0.5 m, the soil had a G of 20 MPa, v of 0.4, unit weight (γ) of 16 kN/m^3 and undrained strength of 100 kPa. The ultimate bearing capacity of the foundation was 522 kN according to Salgado (2008) and the applied vertical load was 118 kN, which provided a theoretical moment capacity according to Deng et al. (2014) of 45.8 kNm.

Four alternative BNWF models are shown in Fig 5, the first model 'OpenSees-TCL-BNWF' is the model from Harden and Hutchinson (2009) implemented within OpenSees, the other three models were implemented using the OpenSeesPy framework. The 'Linear' model had linear elastic springs with zero tension. The 'Elasto-plastic' model used the *Steel01* material model which provided an elastic response until yield, where it has a linear post-yield stiffness, which in this case was set to 0.01. The 'Progressive nonlinear' model used the *SteelMPF* material model, which produces curved transitions between pre- and post-yield load paths, based on curvature parameters R0, a1 and a2, which were set to 2, 0.0 and 0.15 respectively, also having a post-yield

stiffness of 0.01. Note that the spring ultimate load capacity was evenly distributed across all springs based on the bearing capacity equations from Salgado (2008) for all of the OpenSeesPy models.

Figure 5 shows the moment-rotation response of this simple load path. The results clearly illustrate that the OpenSees-TCL-BNWF model over-estimates the moment capacity (due to the tension capacity of the springs), as well as the linear model (due to no yielding of the springs). The other two models provide reasonable estimates of the moment capacity and initial stiffness. The expected uplift response from Cremer et al. (2002) and simplified moment-rotation model from Millen et al. (2020) are also provided as a reference. Note that both OpenSeesPy nonlinear models have higher moments at uplift than Cremer et al. (2002) and less initial nonlinear response that the expression from Millen et al. (2020), although all of these aspects are dependent on the axial load.

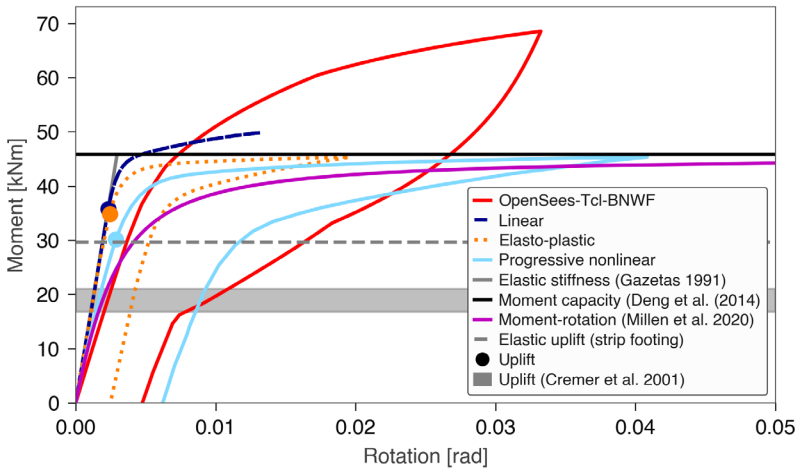

Figure 5: Moment-rotation behaviour of several BNWF models

3.2.1 Combined moment-axial load capacity

To evaluate the moment capacity under different axial load levels, a series of push-over analyses were performed using the progressive nonlinear, and elasto-plastic models. Simulations were performed under constant axial load where the moment demand was increased until failure. The foundation was 4 m in-plane, 7 m out-of-plane, and 1 m deep, and the soil had a G of 80 MPa, ν of 0.3, γ of 16.3 kN/m^3 and internal friction angle of 32°. The moment demand at failure was plotted against the axial load in normalised load space in Figure 6. The ultimate bounding surfaces from Gottardi and Butterfield (1993) and Figini et al. (2012) are both shown. Both BNWF models provide reasonable estimates of the moment capacity across the full range of axial loads, slightly higher than the Gottardi and Butterfield (1993) surface (which is for circular footings) and lower than the Figini et al. (2012) surface.

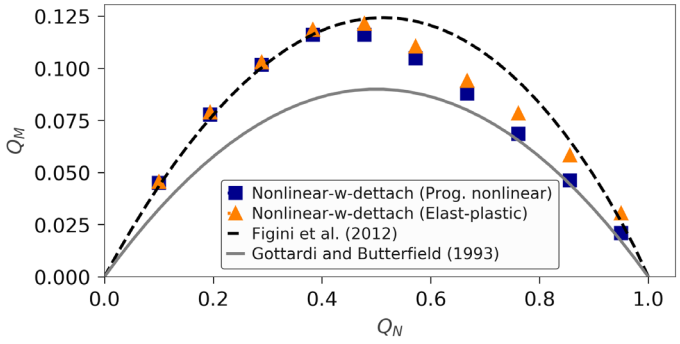

Figure 6: Validation of moment-axial load failure surface

3.3 Vertical load - settlement behaviour

The vertical load versus settlement was investigated by simulating results from a centrifuge experiment, in particular 'Test 2' from Gajan et al. (2003). Only the loading after the fourth cycle was simulated, which covers the loading after some initial static load has been applied. Note that the frictional angle was back calculated using the bearing capacity formula from Salgado (2008) to give 45° and 43.5° for the peak and critical states respectively. Three models were used to simulate the behaviour (Figure 7). The first model used the *SteelMPF* model with R0 of 2, a1 of 0.0, and a2 of 0.15, and computed the bearing capacity using a friction angle, φ, of 43.5 ° and the springs had a post-yield stiffness of 0.001. The second model used the same properties for the SteelMPF model, except the bearing capacity was calculated with an internal frictional angle of 42 ° and a post-yield stiffness of 0.07. The third model used the elasto-plastic response of the *Steel01* model, with an internal frictional angle of 42 ° and a post-yield stiffness of 0.07. The second and third models more accurately depict the response up to the peak response, however, the bearing capacity is not correctly captured compared to the first model. Depending on the expected load paths, the analyst should adjust the ultimate capacity and post-yield stiffness to best capture the most important aspects of the response. Note also that even though the springs in the third model were elasto-plastic, the foundation response produces progressive nonlinear behaviour due to the parabolic distribution of initial stiffness in the springs.

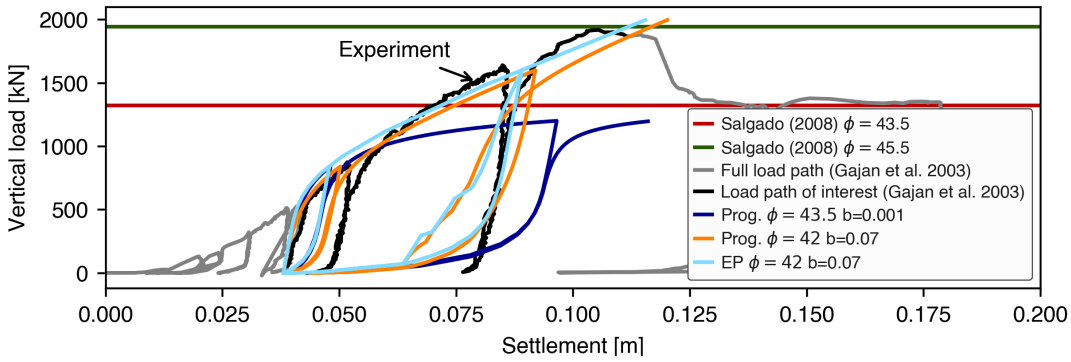

Figure 7: Simulation of vertical load versus vertical displacement compared to experimental results

4 PUSH-PULL ASSESSMENT OF FRAME BUILDINGS

The four storey building designed in the first section was simulated in a push-pull analysis under four different scenarios to investigate the role of SFSI on frame buildings. The first model was for fixed base conditions, while the second and third models assumed no tie beams and the BNWF springs were set to match either the vertical or rotational stiffness. The final model also set the springs to match the vertical stiffness and assumed linear tie beams of 0.6 m deep by 0.8 m wide and a Young's modulus of 25 GPa. The tie beams were modelled as linear elements with a stiffness of 60% of the elastic stiffness. The soil G was assumed to be 20 MPa, and ν was taken as 0.3. The frame was modelled in O3seespy with *ForceBeamColumn* elements, where the beam and column base hinge lengths were 0.4 m, and the remainder of the beams and columns were modelled as elastic elements. The stiffness of the elastic elements was taken as 50% and 40% of the elastic stiffness of the columns and beams respectively, to account for concrete cracking. The beam hinges were modelled with the *Steel01* model with a post-yield stiffness of 0.02 and the moment yield capacity set to the design moment. The column base hinges were modelled with the *ElasticBilin* model with a post-yield stiffness of 0.005 and moment yield capacity equal to the design moment. While the hinge models are simplistic (i.e. columns do not capture moment-axial load interaction), the main findings of this study are not expected to change using more advanced models. In these models the vertical loads were applied at the beam-column joints and centres of the footings, no P-delta effects were considered.

Figure 8a shows the base shear versus roof displacement of the four storey building. It is clear that the global rotation of the foundation, and the local displacements of the footings, softens the response compared to the fixed base model. However, the case where tie beams were used still results in a similar final base shear capacity (and notably less energy dissipation). The lack of tie beams clearly reduced the ultimate base shear resistance of the frame as insufficient moment capacity could develop at the base of the columns. In these analyses matching K_N or K_M made very little difference to the overall response, since the footings had significant nonlinear behaviour (footing uplift and soil yielding). Figure 8b shows the top and bottom moment response of the first storey column that initially decreases in axial load during the push over. Note that even though the top of the column was modelled elastically, in the fixed base model and tie beams model, the moment demand stops increasing at about 200 kNm, since a full beam-sway mechanism has formed. Most concerning for structural assessment is that the models without tie beams produced higher moment demands at the top of the ground storey columns! The reason for this is that there was high local rotation of the footing, which meant that the column inflexion point shifts downwards (to very near the base of the column - see the very low moment demands in the column base for these analyses). In this scenario there is greater potential to create a soft storey mechanism with yielding in the tops of the first storey columns and the full moment capacity of the footings being developed. The reason for the high footing rotations is explained when viewing Figure 8c, when axial load decreases in the exterior footings the footing reaches it moment capacity and with a further reduction in the axial load the moment capacity reduces to near zero. Note that moment capacity reduces to zero in the tie beams model (as the entire foundation rotates and uplifts the external footing), However, the column base moment remains high because of the moment resistance of the tie beams. The greater global foundation rotation in the tie beams model also means that the changes in axial load are more extreme in the external footings, and even causes a reduction in axial load in the central footing. The increase in axial load in the central footing due to beam yielding for the no tie beams model was also clearly observed, however, it was full restored once the beam hinges were yielded back in the opposite direction.

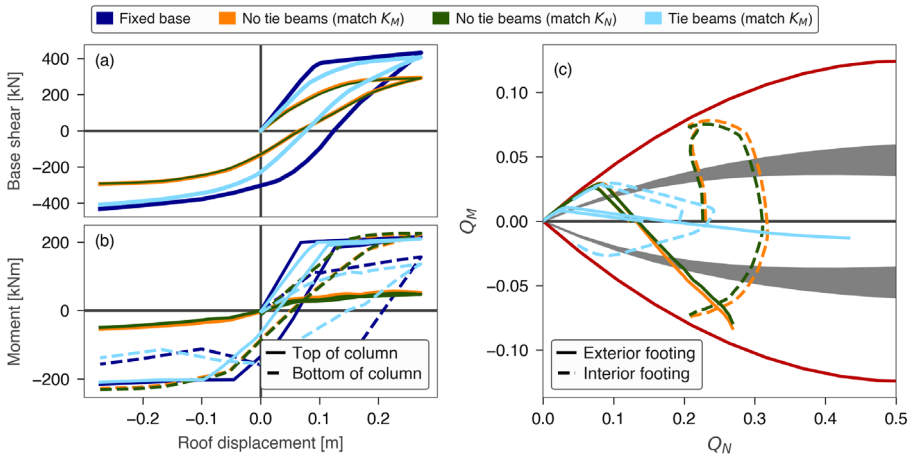

Figure 8: Push-pull analyses of a 4-storey frame building a) base shear versus roof displacement, b) ground floor moment demand versus roof displacement, c) footing moment and axial load

From the simple study produced here it is clear that the role of SFSI in the assessment of frame buildings is more complex than for simple linear systems. However, with careful modelling of the soil-foundation interface the influence of soil-foundation-structure interaction can and should be accounted for within the seismic assessment of a building.

5 OUTSTANDING ISSUES

While this paper provides some guidance on implementing and validating BNWF models, there are still several outstanding issues. The simulation of hysteretic energy dissipation needs to be validated, as well as the

modelling and combination of hysteretic and radiation damping under dynamic loading. The presented modelling efforts assumed that each footing was completely independent, however, it could be expected that loads in one footing would influence the response in other footings (through the soil) if they were close to each other. The role of shear demand on the footing, and the role of soil contact along the sidewalls of embedded footings, on the moment and vertical response should be quantified. The estimation of the soil shear modulus is not trivial, given that soil stiffness is stress- and strain-dependent, the potentially large variation in axial load makes this problem more complex than foundations under purely moment loading. Additionally, the estimation of the soil shear modulus under seismic excitation is complicated by the substantial shear strains induced by the seismic waves.

6 CONCLUSIONS

This paper provides guidance on the development, validation and implementation of BNWF models for SFSI assessment of frame buildings. The load paths on footings depend on the building geometry and foundation sizes, however, a significant variation in both moment and axial load under seismic excitation can be expected. In this paper a parabolic spring stiffness distribution was proposed to provide suitable behaviour across a range of load paths. The rotational or vertical stiffness could be matched, however, as the foundation aspect ratio tended towards a strip foundation, a compromise in one mode is needed. The proposed BNWF was able to reasonably capture the expected moment-axial load failure surface and vertical load versus displacement response, however, could not capture both the peak and critical vertical load response using a single set of parameters. The BNWF should not be used to estimate the loads within the foundation element, and further calibration is required to accurately simulate the hysteretic energy dissipation and residual deformations. The simulation of a push-pull analysis of a frame building highlighted that both the global foundation rotation, and the local footing deformations, can significantly influence the backbone response of the building. The frame building without tie beams also had larger demands at the top of the ground floor columns than the equivalent fixed base model. The frame with tie beams had significantly larger changes in axial load in the footings than the model without tie beams and changes in axial load significantly influenced the foundation moment capacity. Overall the BNWF model can be used for the seismic assessment of frames but careful consideration of the load paths of the footings is needed, and appropriate modelling of the foundation tie beams is required.

7 ACKNOWLEDGEMENTS

The authors would like to acknowledge the financial support provided through the Built Environment theme of the Resilience to Natures Challenges project.

8 REFERENCES

ATC-40. 2008. Seismic evaluation and retrofit of concrete buildings. pages 1–334. *Applied Technology Council.*

Brinch Hansen J. 1970. A revised and extended formula for bearing capacity. *The Danish Geotechnical Institute*, Bulletin No. 28.

Cremer, C., Pecker, A., & Davenne, L. 2001. Cyclic macro-element for soil-structure interaction: material and geometrical non-linearities. *International Journal for Numerical and Analytical Methods in Geomechanics*, 25(13):1257–1284.

Cremer, C., Pecker, A., & Davenne, L. 2002. Modelling of nonlinear dynamic behaviour of a shallow strip foundation with macro-element. *Journal of Earthquake Engineering*, Vol 6(2):175–211.

Cubrinovski, M., Bradley, B.A., Wotherspoon, L.M., Green, R., Bray, J D., Wood, C., Pender, M.J., Allen, J., Bradshaw, A., & Rix, G. 2011. Geotechnical Aspects of the 22 February 2011 Christchurch Earthquake. *Bulletin of the New Zealand Society for Earthquake Engineering*, Vol 44(4).

Deng, L., Kutter, B.L., & Kunnath, S.K. 2014. Seismic Design of Rocking Shallow Foundations: Displacement-Based Methodology. *Journal of Bridge Engineering*, 19(11):04014043–11.

Figini, R., Paolucci, R., & Chatzigogos, C.T. 2012. A macro-element model for non-linear soil-shallow foundation-structure interaction under seismic loads: theoretical development and experimental validation on large scale tests. *Earthquake Engineering & Structural Dynamics*, Vol 41(3):475–493.

Gajan, S., Phalen, J.D., & Kutter, B.L. 2003. Soil-Foundation-Structure Interaction: Shallow Foundations, Centrifuge Data Report For SSSG02. pages 1–109.

Gazetas, G. 1991. Formulas and Charts for Impedances of Surface and Embedded Foundations. *Journal of Geotechnical Engineering*, Vol 117(9):1363–1381.

Gottardi, G. & Butterfield, R. 1993. On the Bearing Capacity of Surface Footings on Sand Under General Planar Loads. *Soils and foundations*, Vol 33(3):68–79.

Harden, C.W. & Hutchinson, T.C. 2009. Beam-on-Nonlinear-Winkler-Foundation Modeling of Shallow, Rocking-Dominated Footings. *Earthquake Spectra*, Vol 25(2):277–300.

MBIE, EQC, NZSEE, SESOC, & NZGS. 2017. Geotechnical Considerations. In The Seismic Assessment of Existing Buildings, pages 1–76. www.EQ-Assess.org.nz.

McKenna, F., Scott, M.H., & Fenves, G.L. 2010. Nonlinear Finite-Element Analysis Software Architecture Using Object Composition. *Journal of Computing in Civil Engineering*, Vol 24(1):95–107.

Millen, M.D.L., Pampanin, S., & Cubrinovski, M. 2020. An integrated performance-based design framework for building-foundation systems. *Earthquake Engineering & Structural Dynamics*, Vol 172(1):1–21.

Millen, M.D.L., Pampanin, S., Cubrinovski, M., & Carr, A.J. 2016. A performance assessment procedure for existing buildings considering foundation deformations. In *2016 NZSEE Conference*, pages 1–8.

Salgado, R. 2008. The Engineering of Foundations. New York: *McGraw Hill*, ISBN: 0072500581. Sullivan, T. J., Priestley, M. J. N., and Calvi, M. G. 2012. DBD12: A model code for the displacement-based

seismic design of structures. Italy: *IUSS Press*.

Wotherspoon, L.M. 2009. Integrated modelling of structure-foundation systems. PhD thesis, *The University of Auckland*.

Zhu, M., McKenna, F., & Scott, M.H. 2018. OpenSeesPy: Python library for the OpenSees finite element framework. *SoftwareX*, Vol 7:6–11.